Investigation of UWB antenna on-chip integration in CMOS process towards energy-autonomous implantable biosensors

Martin Kovac*, Viera Stopjakova, Gabriel Nagy, and Daniel Arbet

Institute of Electronics and Photonics, Slovak University of Technology,
Ilkovicova 3, 81216 Bratislava, Slovakia
{martin_kovac,viera.stopjakova,gabriel.nagy,daniel.arbet}@stuba.sk
http://uef.fei.stuba.sk/uef/en

Abstract. This paper discusses about the possibility of ultra-wideband (UWB) antenna integration into an integrated circuit (IC) chip together with other parts of the electronics system in a standard CMOS manufacturing technology. Recently, researches has come to the conclusion that UWB technology, and its lower band of the frequency range in particular, represents a very attractive communication option for implantable biosensors. The presence of human tissue significantly influences characteristics of an electromagnetic radiator at low frequency that benefits in the integration capability. Therefore, the feasibility analysis of the anntena integration taking the traditional planar spiral square Archimedean antenna (PSSAA) incorporating the shielding layer is addressed, and possibilities of the radiation improvement in the future research are discussed in this paper.

Keywords: UWB antenna, CMOS standard process, implantable biosensors, spiral antenna

1 Introduction

In the last few decades, the popularity of communication technologies utilizing the wide band of radio spectrum increased significantly. This is a consequence of requirements for high data rate capability (*Gbps* order of magnitude), where the most attractive applications can be found in mobile communication and high–quality multimedia data transfer. In the present time, the evolution of wireless access technologies is about to reach its fifth generation (5G) working in millimeter waves (mmWave), where communication about 28 GHz and 38 GHz center frequencies introduces the most promising choose [1]. On the other hand, for communications, computing and consumer electronics that require wireless systems delivering multiple gigabits of data throughput operating on license-exempt radio spectrum, frequencies in 60 GHz range are benefited [2]. Favor of high frequency for communication predetermines the possibility of antenna integration directly on a chip, as will be demonstrated in Section 2. However, the utilization of such high frequencies is completely infeasible for deep-implanted biosensors. These frequencies can be useful exclusively in subcutaneous applications [3].

Raul Chavez–Santiago et al. investigated the possibility of deploying the UWB technology in deep implantable sensors [4]. It has been observed that this technology (especially lower frequency band) for human tissue with a thickness of less than 100 mm shows comparable values of path loss ($\leq$ 60 dB with the predicted root–mean–square delay spread values below 1 ns for vertical polarization) to those achieved for medical implant communication service (MICS) band. The most recent publication [5] confirms the predicted applicability of the impulse radio UWB (IR–UWB) in living tissue, where the bit–error–rate (BER) of 10^{-2} at 120 mm distance from an animal surface was achieved. This proves the suitability of IR–UWB technology deployment (particularly lower frequency band starting from 3.1 GHz) also in deep implantable biosensor applications.

Despite the well-explored IR–UWB transmitter configuration, the challenge to find the most suitable antenna solution still persist. This issue takes on the seriousness with the intention to integrate the UWB antenna on chip together with other electronics, where reasonable antenna dimensions and radiation characteristics are targeted and the idea is supported by exploitation of the high permittivity tissue.

Section 2 is dedicated to a brief survey of ultra-wideband antennas, e.i. $f_{max} - f_{min} \geq$ 500 MHz realized in a standard CMOS process, where f_{max} and f_{min}) are high and low antenna corner frequencies, respectively and their difference represents the effective frequency band of an antenna.

2 Previous work

Several antenna design contributions in a standard CMOS process, especially for frequency of 60 GHz and above have been presented so far. Here, the

ultra-wideband properties of the antenna can be achieved much easier also using standard narrow-band antennas types such as monopole, dipole, slot and patch antennas [6]. Primarily, this phenomenon is due to tighter antenna coupling with lossy substrate, which significantly modifies near-field radiation and influences the radiation characteristics. Naturally, there exist a lot of innovative design techniques such as bond–wire like antenna, (cavity, reflector, dielectric, artificial magnetic conductor, CMOS-MEMS, etc.)–based antenna and antenna arrays [7]–[12]. On the other hand, regarding the lower frequencies, the research is much poorer because of unacceptably high price in terms of the chip total dimensions. If we look closer at the IR-UWB frequency band of interest, e.i $3.1-10.5\,GHz$, the overview presented in Table 1. can be carried out.

Table 1. On–chip antenna review for IR-UWB frequency band realized in a standard CMOS process

	[13]	[14]	[15]	[16]	[17]
antenna type	multiturn loop dipole	spiral-slot	triple-resonance dipole	mono-pole	meander dipole
lower freq. [GHz]	3.8	≈8.5	3.5	8	3
freq. band [GHz]	2	≈2	21.7	2	–
gain [dBi]	–	-10	≈-16.3*	-27.4	–
shielding	no	yes	no	no	no
max. dimension [mm]	3	0.78	4.2	3.37	4

* calculated from [18] considering perfect antenna matching.

Most of the referred antennas have the spiral structure leading to significant improvement of the antenna form factor, and particularly, works presented in [14] and [15] represent theoretically a promising solution for the research area of implantable biosensors. However, [14] suffers from excessively narrow frequency band, and the low frequency corner persists still too high that can be a problem in the case of replacement of power-hungry IR-UWB receiver by a low-power asynchronous wake–up receiver working in industrial, scientific and medical (ISM) radio bands ($2.45\,GHz$, $5.8\,GHz$). Nevertheless, this solution is still unique in terms of lossy substrate isolation by a shielding layer, resulting in the antenna gain improvement. Unlike the previous case, the antenna design presented in [15] has mightily wider frequency band in opposite the low antenna gain (calculated for $10\,GHz$ frequency) and worse form factor. Also [13] and [17] presented attractive solutions in terms of working frequency and reasonable form factor, however, the antenna gain between $-25\,dBi$ and $-30\,dBi$ is expected.

However, it should be noted that so far no on-chip implementation of an antenna in a standard CMOS process has been analyzed in conjunction with the implantable biosensors and living tissue interaction. With the fast development of smart biosensors and implants using wireless communication, this option becomes more attractive. Moreover, since implantable biosensors are very complex heterogeneous systems often vertically integrated into a 3D vertical stack, the chip area sacrificed for the antenna implementation could be effectively utilized for electronics and other parts of the system, if a proper antenna design and shielding with reasonable antenna properties will be incorporated.

3 Designed IR-UWB antenna

In our research, we focus on traditional planar spiral square Archimedean antenna (PSSAA), as one of the most promising ultra-wideband antenna solutions for on-chip implementation done using in a standard $90\,nm$ CMOS process. In general, the PSSAA is considered as being a naturally ultra-wideband antenna with circular polarization, good directional ability and favourable form factor (FF), i.e $FF \approx (1.25/4)\lambda_{max}$ in traditional antenna design, where λ_{max} corresponds to low-band frequency. In addition, the active radiation area is located directly between the adjacent wires. However, there is a presumption that such an antenna will require larger area with respect to solutions presented in Table 1. This disadvantage can be partially reduced by a novel design concept introduced in [19], where the presence of a shielding layer is necessary to protect the electronics from the antenna electromagnetic interaction.

The initial simulations were performed using 12-turns PSSAA located on the top layer (AL RDL layer in the selected technology) with $12\,\mu m$ width and incorporating the fully filled shielding layer realized using the UTM layer (layer located just below the AL RDL layer). The number of turns was retained and only w_c (parameter directly defining FF [19] was varied in further simulations. Results achieved within this analysis are depicted in Fig.1, where an important observation can be made, e.i. the antenna gain increases with its dimensions. However, the saturated trend of individual curves can be also observed. This is a consequence of the total loss of mutual coupling between adjacent wires due to the shielding layer presence. For this reason, the symmetry edge coupled microstrip transmission line (SECMTL) (as the PSSAA at the

simplified first glance looks like) incorporating the inhomogeneous substrate is investigated.

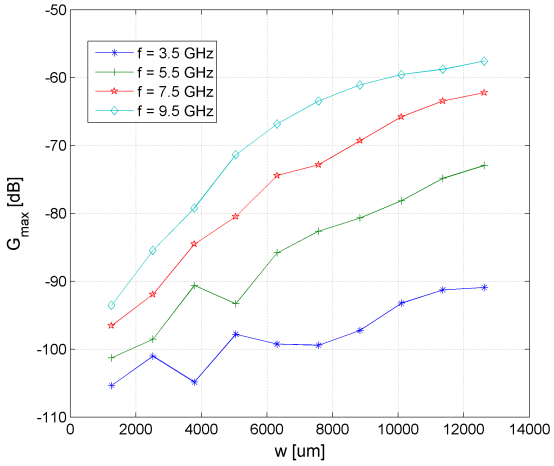

Fig. 1. Antenna gain versus the maximum antenna dimensions.

3.1 Edge coupled microstrip transmission line investigation

For better understanding of the behaviour of PSSAA designed in TSMC CLM90 standard CMOS process and investigation of the effect of shielding layer, simulations of the SECMTL coupling coefficient k was performed as the most testifying parameter of mutual coupling. Also the differential effective permittivity ε_{eff} was listed for clearness. The achieved simulation results for the low corner frequency are demonstrated in Fig.2. Parameter k is defined as

$$k = \frac{Z_{o,e} - Z_{o,o}}{Z_{o,e} + Z_{o,o}} = \frac{4Z_{o,cm} - Z_{o,diff}}{4Z_{o,cm} + Z_{o,diff}}, \qquad (1)$$

where $Z_{o,cm}$ and $Z_{o,diff}$ are common and differential characteristic impedances of the SECMTL, respectively.

From these two graphs, one can observe that there exists only a limited area (bottom–left corner), where the coupling coefficient is better than 10%. This area is characterized by small wire width and space between individual wires that converged to the limits of TSMC CLM90 standard CMOS process dimensions (3 μm for width and 2 μm for space). Unfortunately, too small dimensions of the antenna wires can lead to high parasitic resistance, and also the yield of integrated circuit production can be affected. Obviously, this is the reason why gain shown in Fig. 1 is considerably small (valid for 12 μm constant width and $\leq$ 12μm varying space of individual antenna wires). From Fig. 2b we can also conclude that by increasing the gap between wires while maintaining the number of turns and keeping the width constant, the differential permittivity increases implicated the closer coupling with the shield layer. Rapid decrease of ε_{eff} towards lower wire dimensions, represents the "hooking" of the antenna wires radiation with each other leading to improvement of radiation characteristics of PSSAA.

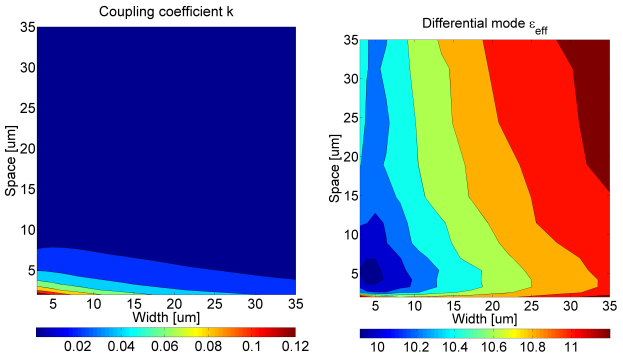

Fig. 2. Coupling coefficient k (left) and differential effective permittivity ε_{eff} (right) as a function of wire width and wire space (with the absence of human tissue; valid for 3.1 GHz).

4 Discussion and conclusion

This paper presents the research that is based on our previous work [19], where the novel concept of a planar fully integrated implantable biosensors was introduced. Preliminary simulation results showed unsatisfying antenna radiation characteristics, especially antenna gain, although ultra-wideband behaviour was demonstrated. To improve the antenna gain, the SECMTL analysis including properties of TSMC CLM90 standard CMOS process was performed. It has been demonstrated that realization of the PSSAA on the top layer and using a shielding layer just under it did not lead to an acceptable solution. To overcome this undesired behaviour and ensure the possibility of future PSSAA optimization, we suggest relocation of the shielding layer to one layer below, in particular, to 3XTM layer that has comparable resistivity parameter to UTM layer. This solution increases the space between antenna and the shielding layer to slightly more than 3.4 μm, which offers possibilities for antenna radiation improvement. The profit of this approach is demonstrated in Fig.3. where antenna gain increase from -93.5 dBi to -73.9 dBi. We must note that present of effective radiation shielding is observed at higher antenna dimensions [19].

Acknowledgments. This work was supported in part by FP7 ICT Project SMAC (Agr. No. 288827) and Competence Center for SMART Technologies for Electronics and Informatics Systems and Services (ITMS 26240220072) funded by the R&D Operational Programme from the ERDF.

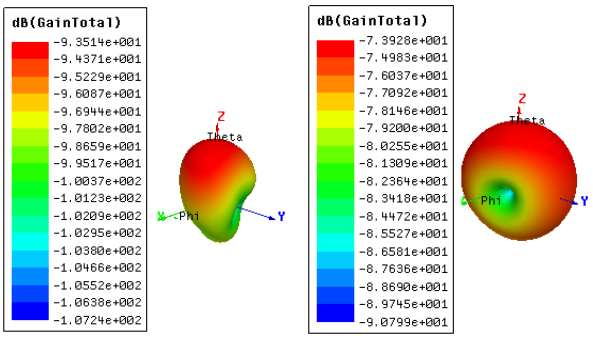

Fig. 3. Demonstration of PSSAA antenna radiation pattern improvement before (left) and after (righ) the shielding layer relocation ($w_c = 1262\ \mu m$, $f = 9.5\ GHz$).

References

1. Rappaport, T.S.; Shu Sun; Mayzus, R.; Hang Zhao; Azar, Y.; Wang, K.; Wong, G.N.; Schulz, J.K.; Samimi, M.; Gutierrez, F., "Millimeter Wave Mobile Communications for 5G Cellular: It Will Work!," Access, IEEE , vol.1, no., pp.335,349, 2013
2. European Telecommunications Standards Institute, "Electromagnetic compatibility and Radio spectrum Matters (ERM); Technical characteristics of multiple gigabit wireless systems in the 60 GHz range," European Telecommunications Standards Institute, ETSI-TR-102-555 V1.1.1, 2007. [Online]. Available: http://www.etsi.org. [Accessed: Oct. 12, 2014].
3. Ahmed, Y.; Hao, Y.; Parini, C., "A 31.5GHz Patch Antenna Design for Medical Implants," International Journal of Antennas and Propagation, vol. 2008, Article ID 167980, 6 pages, 2008.
4. Chavez-Santiago, R.; Sayrafian-Pour, K.; Khaleghi, A.; Takizawa, K.; Jianqing Wang; Balasingham, I.; Huan-Bang Li, "Propagation models for IEEE 802.15.6 standardization of implant communication in body area networks," Communications Magazine, IEEE , vol.51, no.8, pp.80-87, 2013.
5. Anzai, D.; Katsu, K.; Chavez-Santiago, R.; Qiong Wang; Plettemeier, D.; Jianqing Wang; Balasingham, I., "Experimental Evaluation of Implant UWB-IR Transmission With Living Animal for Body Area Networks," Microwave Theory and Techniques, IEEE Transactions on , vol.62, no.1, pp.183,192, Jan. 2014
6. Huang, K.-K.; Wentzloff, D.D., "60 GHz on-chip patch antenna integrated in a $0.13 - \mu\ m$ CMOS technology," Ultra-Wideband (ICUWB), 2010 IEEE International Conference on , vol.1, no., pp.1,4, 20-23 Sept. 2010
7. Kuo-Ken Huang; Wentzloff, D.D., "60 GHz wirebond helical antennas in 130 nm CMOS technology," Antennas and Propagation Society International Symposium (APSURSI), 2012 IEEE , vol., no., pp.1,2, 8-14 July 2012
8. Rui Wu; Wei Deng; Sato, S.; Hirano, T.; Ning Li; Inoue, T.; Sakane, H.; Okada, K.; Matsuzawa, A., "A $17 - mW5 - Gb/s60 - GHz$ CMOS transmitter with efficiency-enhanced on-chip antenna," Radio Frequency Integrated Circuits Symposium, 2014 IEEE , vol., no., pp.381,384, 1-3 June 2014
9. Smolders, A.B.; Johannsen, U.; Liu, M.; Yu, Y.; Baltus, P.G.M., "Differential 60 GHz Antenna-on-Chip in mainstream 65 nm CMOS technology," Antennas and Propagation Society International Symposium (APSURSI), 2014 IEEE , vol., no., pp.356,357, 6-11 July 2014
10. Debin Hou; Yong-Zhong Xiong; Wang-Ling Goh; Sanming Hu; Wei Hong; Madihian, M., "$130 - GHz$ On-Chip Meander Slot Antennas With Stacked Dielectric Resonators in Standard CMOS Technology," Antennas and Propagation, IEEE Transactions on , vol.60, no.9, pp.4102,4109, Sept. 2012
11. Xiao-Yue Bao; Yong-Xin Guo; Yong-Zhong Xiong, "60-GHz AMC-Based Circularly Polarized On-Chip Antenna Using Standard $0.18 - \mu m$ CMOS Technology," Antennas and Propagation, IEEE Transactions on , vol.60, no.5, pp.2234,2241, May 2012
12. Chun-Chi Lin; Sheng-Chi Hsieh; Chin-Yen Huang; Chia-Chan Chang, "Frequency-tunable CMOS-MEMS slot antenna," Antennas and Propagation Society International Symposium (APSURSI), 2012 IEEE , vol., no., pp.1,2, 8-14 July 2012
13. Radiom, S.; Baghaei-Nejad, M.; Aghdam, K.; Vandenbosch, G.A.E.; Li-Rong Zheng; Gielen, G.G.E., "Far-Field On-Chip Antennas Monolithically Integrated in a Wireless-Powered $5.8 - GHz$ Downlink/UWB Uplink RFID Tag in $0.18 - \mu m$ Standard CMOS," Solid-State Circuits, IEEE Journal of , vol.45, no.9, pp.1746,1758, Sept. 2010
14. Behdad, N.; Dan Shi; Wonbin Hong; Sarabandi, K.; Flynn, M.P., "A $0.3mm^2$ Miniaturized X-Band On-Chip Slot Antenna in 0.13 m CMOS," Radio Frequency Integrated Circuits (RFIC) Symposium, 2007 IEEE , vol., no., pp.441,444, 3-5 June 2007
15. Kikkawa, T., "Gaussian monocycle pulse CMOS transmitter with on-chip integrated antenna and high-k dielectric slab waveguide," Solid-State and Integrated Circuit Technology (ICSICT), 2012 IEEE 11th International Conference on , vol., no., pp.1,4, Oct. 29 2012-Nov. 1 2012
16. Kulkarni, V.V.; Muqsith, M.; Niitsu, K.; Ishikuro, H.; Kuroda, T., "A 750 Mb/s, 12 pJ/b, 6-to-10 GHz CMOS IR-UWB Transmitter With Embedded On-Chip Antenna," Solid-State Circuits, IEEE Journal of , vol.44, no.2, pp.394,403, Feb. 2009
17. Sasaki, N.; Kimoto, K.; Moriyama, W.; Kikkawa, T., "A Single-Chip Ultra-Wideband Receiver With Silicon Integrated Antennas for Inter-Chip Wireless Interconnection," Solid-State Circuits, IEEE Journal of , vol.44, no.2, pp.382,393, Feb. 2009
18. Kubota, S.; Toya, A.; Sugitani, T.; Kikkawa, T., "$5 - Gb/$s and $10 - GHz$ Center-Frequency Gaussian Monocycle Pulse Transmission Using $65 - nm$ Logic CMOS With On-Chip Dipole Antenna and High-(kappa) Interposer," Components, Packaging and Manufacturing Technology, IEEE Transactions on , vol.4, no.7, pp.1193,1200, July 2014
19. Kovac, M.; Nagy, G.; Stopjakova, V.; Arbet, D., "Simulation of CMOS Integrated UWB Antenna for Implantable Biosensors," 22nd Telecommunications Forum (TELFOR 2014), Belgrade (Serbia), 25-27 November 2014, [Paper Accepted]